Electronic Supporting Information for

Ultrasensitive Detection of Nitrite through Implementation of *N*-(1-Naphthyl)ethylenediamine-Grafted Cellulose into a Paper-Based Device

Teresa L. Mako, Adelaide M. Levenson, and Mindy Levine*

Department of Chemistry, University of Rhode Island, 140 Flagg Road, Kingston, RI 02881 USA

Department of Chemical Sciences, Ariel University, 65 Ramat HaGolan Street, Ariel, Israel

Table of Contents

General Considerations

All chemicals and cellulose products were purchased through Fisher Scientific and Millipore Sigma. 1,8-diazabicyclo[5.4.0]undec-7-ene (DBU) was purified via distillation under dynamic vacuum at 90 °C; all other materials were used as received. Synthetic freshwater was made following the EPA standard procedures.[1] Synthetic seawater with a salinity of 30.5 ppt was prepared using Red Sea Coral Pro Salt mix by dissolving 33.4 g of the salt mix in 1 L of ultrapure water. An ICP-MS analysis of the salt mixture was provided by Red Sea (Figure S1). Water from the Sargasso Sea (located in the North Atlantic near Bermuda, a typically low-nutrient environment[2]) was collected by Dr. Bethany Jenkins and coworkers from the Department of Cell and Molecular Biology at the University of Rhode Island, and filtered through a 0.2 μm filter to remove organic matter prior to usage.

Name of product tested: Coral Pro Salt

Batch number: 1903170115

Tested element	Units	Acceptable Range	Batch Analysis
pH		8.2-8.5	8.30
Total Alkalinity	meq/l	4.15-4.45	4.24
Calcium | Ca	mg/l	450-480	466.49
Magnesium | Mg	mg/l	1350-1430	1389.82
Sulfur | S	mg/l	870-930	883.00
Potassium | K	mg/l	385-415	393.43
Bromine | Br	mg/l	60-70	63.43
Strontium | Sr	mg/l	8.5-10.5	10.11
Boron | B	mg/l	4.45-4.95	4.73
Total ammonium | NH4/NH3	mg/l	≤0.1	≤0.1
Nitrate | NO3	mg/l	≤0.3	≤0.3
Phosphate| PO4	mg/l	≤0.03	≤0.03

Figure S1. ICP analysis for the Coral Pro Salt mix used for salinity studies. All numbers are based on a 35 ppt solution. Provided by Red Sea MyBatch.

Colorimetric measurements were conducted by obtaining digital images of the used sensors with an EPSON V19 Perfection flat-bed scanner and the images were analyzed using ImageJ software (https://imagej.nih.gov/ij/download.html) on an 8-bit color scale (white = 255 a.u., black = 0 a.u.). Using ImageJ, the detection zone coloration was separated into average RGB channels and converted into Normalized Green Value (NGV) by dividing the Green Value (the color value that changed the most with an increase in magenta color) by Red Value (the color value that changed the least with an increase in magenta color). Lower Green Values and Normalized Green Values correspond to darker magenta color, i.e. more azo dye formed. Pixel standard deviation (PSD), a measure of pixel color homogeneity[3] that was provided by the ImageJ program, was also used as a metric for analysis. All colorimetric measurements were repeated 3-6 times to ensure precision of the colorimetric technique.

Fluorimetric measurements were conducted using a BioTek Instruments Synergy H1 microplate reader with the following parameters: excitation: 300 nm, emission: 340 to 575 nm, gain: 45; data interval: 1 nm, read height: 10.68 mm. Six mm diameter pieces of the functionalized paper were cut using a hole punch, then placed in a BioTek 96 well plate for analysis. Each sample was measured four times, from which averages of fluorescence integration were calculated and then normalized for further comparisons. Fluorescence integrations were performed using OriginPro 2018 or OriginPro 2019. Higher fluorescence integration values correspond to more *N*-(1-naphthyl)ethylenediamine bound to the cellulose substrate. All fluorimetric experiments were repeated with at least three paper samples to ensure the reproducibility of the functionalization techniques.

The paper-based devices were designed using Adobe Illustrator and printed using a Xerox ColorQube 8580 wax printer. Fellowes 3mil self-adhesive laminate sheets and FLEXcon FLEXmount SELECT DF051521 clear 0.5 poly perm adhesive/ double faced liner were cut to the desired sizes using a Graphtec CE6000-40 cutting plotter.

Device Application and Architecture Optimization

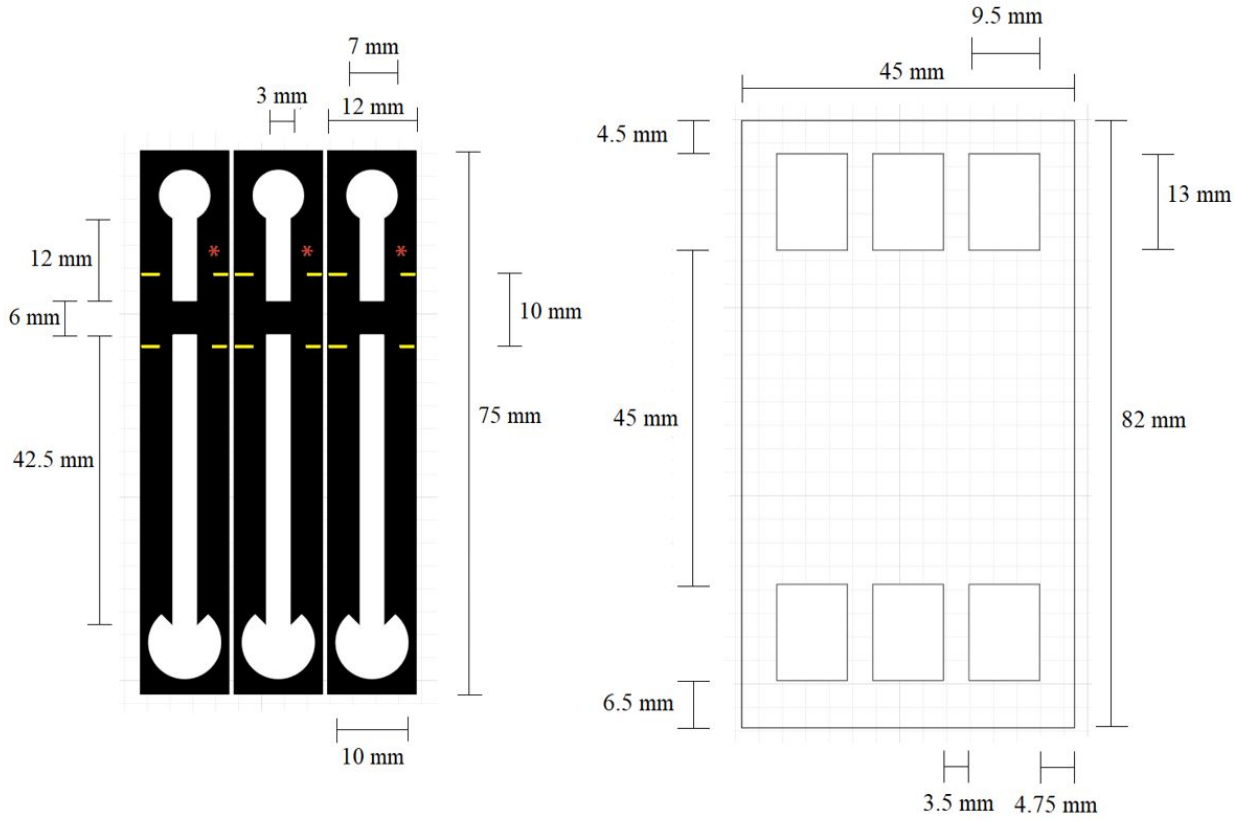

Figure S2. Dimensions for wax printed device (left image) and cut laminate (right image) for triplicate devices.

Architecture Optimization

Device performance was analyzed by examining the colorimetric response (as Green Value or Normalized Green Value) of the devices to three different nitrite concentrations (10, 40, and 200 μM). Average and standard deviations of the Green Values (across three measurements) were considered when comparing the devices as well as the general evenness of the coloration of the detection zone (measured as PSD).

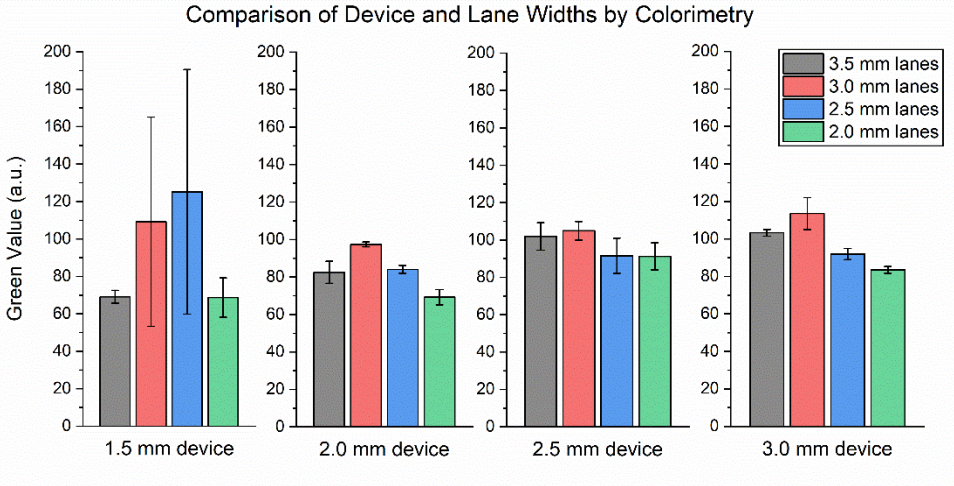

Figure S3. Comparison of four device channel widths, 1.5, 2.0, 2.5, and 3.0 mm, with four functionalized paper lane widths, 2.0, 2.5, 3.0, and 3.5 mm, by colorimetry using 200 μM nitrite. A device with a 3.0 mm wide channel paired with a lane 2.5 mm wide gave the most optimal coloration (darkness and evenness). 1.5 mm and 2.0 mm device widths, and 2.0 mm lane widths, were eliminated because the detection zone was too small to be accurately characterized visually, and 1.5 mm devices gave highly variable coloration of the detection zone. Sulfanilamide was dissolved and deposited using 1.0 M phosphoric acid rather than 1.0 M HCl.

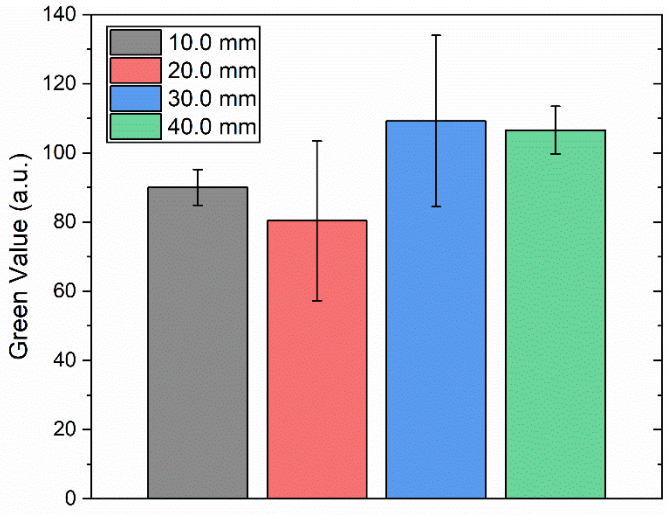

Figure S4. Comparison of the distance of the detection zone from the sample loading zone by colorimetry using 200 μM nitrite. A 10 mm distance was chosen for the optimal device construction. Sulfanilamide was dissolved and deposited using 1.0 M phosphoric acid rather than 1.0 M HCl.

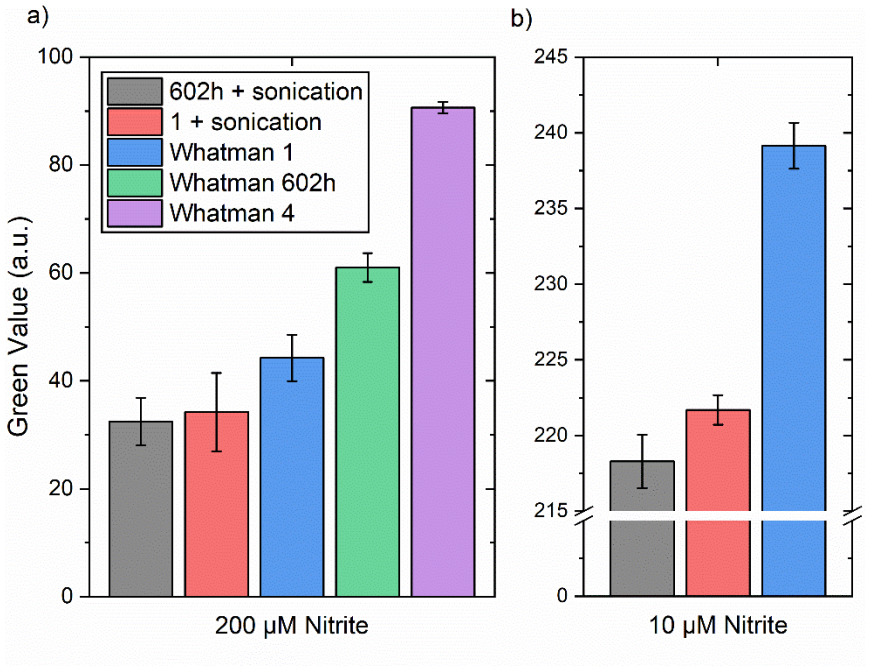

Figure S5. Colorimetric comparison of paper type and sonication conditions at: a) 200 µM nitrite and b) 10 µM nitrite.

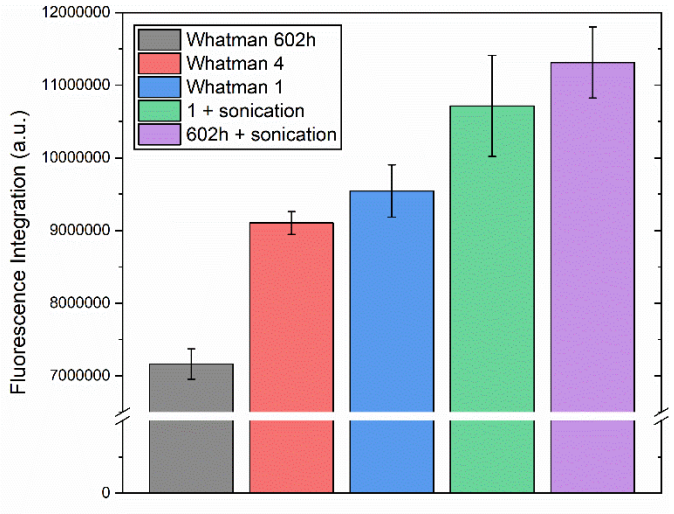

Figure S6. Comparison by fluorescence spectroscopy of types of paper with and without sonication conditions.

Functionalization of Cellulose

Initial Functionalization Conditions

The paper was patterned using a wax printer with a 10 mm x 10 mm wax square with a 6 mm diameter hydrophilic circle in the center. The wax was melted in a 120 °C oven for 2.5 minutes. To an Erlenmeyer flask bearing a 24/40 ground glass joint and a stir bar was added 50 mg of the patterned paper, *N*-(1-naphthyl)ethylenediamine (0.25 – 2.0 mass equiv. to cellulose) and acetonitrile (to achieve a concentration of 0.022 M of *N*-(1-naphthyl)ethylenediamine). 1,8-Diazabicyclo[5.4.0]undec-7-ene (1.1 - 6.0 mol. equiv. to *N*-(1-naphthyl)ethylenediamine) was added and the solution was heated to 50 °C for 30 minutes with gentle stirring at 100 rpm. Epichlorohydrin (1.0 – 4.0 mol equiv. to *N*-(1-naphthyl)ethylenediamine) was then added, a condenser was attached to the Erlenmeyer flask, and the solution was heated to 50 °C for a specified amount of time (1 - 72 hr). After the required time period, the solution was cooled to room temperature. The supernatant was decanted, and the functionalized paper was washed with acetonitrile (2x), distilled water (2x), 1.0 M HCl (2x, 1 min of gentle stirring each), and distilled water (4x). The functionalized paper was collected on a Buchner funnel and vacuum was pulled through for 30 minutes. The paper was further dried in an oven at 50 °C for 30 minutes, then stored in a capped vial away from direct light.

Colorimetric Qualification of Functionalization

A rudimentary device, shown in Figure S7, was constructed for initial quantitation. The functionalized paper circle was adhered using double sided tape to the location shown by the yellow reference lines. 5 µL of 50 mM sulfanilamide solution (8.6 mg per mL of 1.0 M citric acid) was added to the functionalized paper and allowed to dry for 30 minutes. 50 µL of nitrite sample solution (0.3 mM) was applied to the sample loading zone and the sensor readout was allowed to develop for 30 minutes before image collection and analysis. Comparisons were conducted using Green Value or Normalized Green Value.

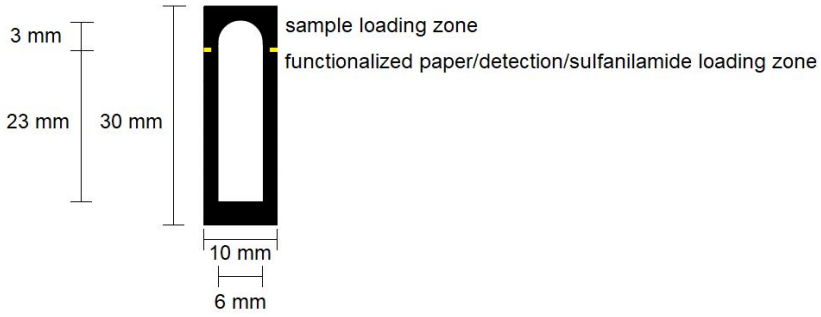

Figure S7. Simple wax-printed device for initial colorimetric analyses

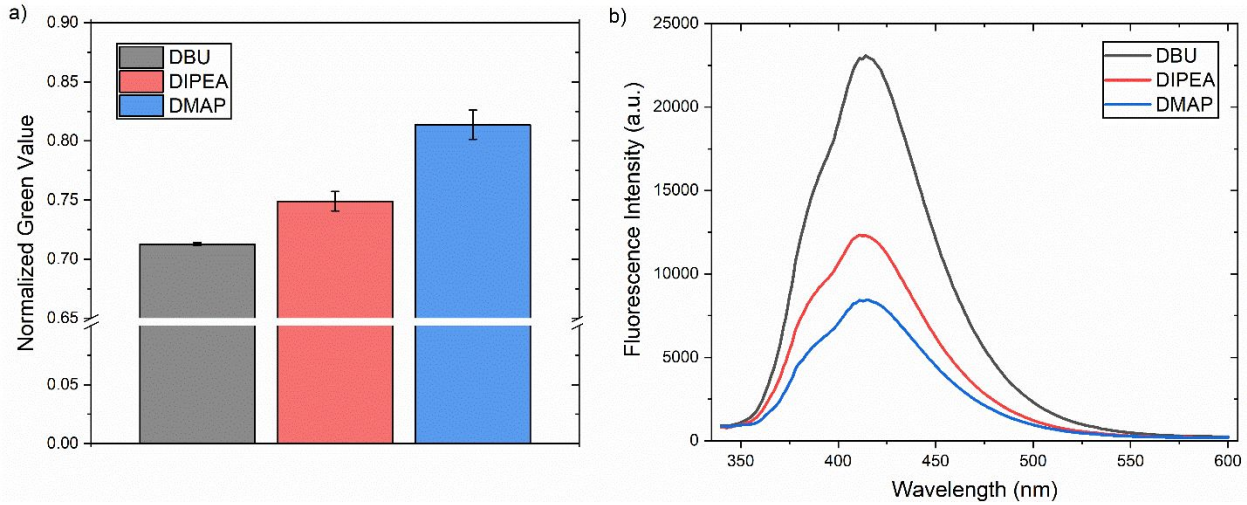

Figure S8. Comparisons of bases used for the deprotonation of *N*-(1-naphthyl)ethylenediamine and cellulose by a) colorimetric analysis and b) fluorescence spectroscopy. For colorimetric comparison, functionalized paper was treated with 300 µM sodium nitrite solution in ultrapure water. DBU: 1,8-diazabicyclo[5.4.0]undec-7-ene; DIPEA: *N,N*-diisopropylethylamine; DMAP: 4-dimethylaminopyridine. Bars indicate error, i.e. standard deviation from three measurements.

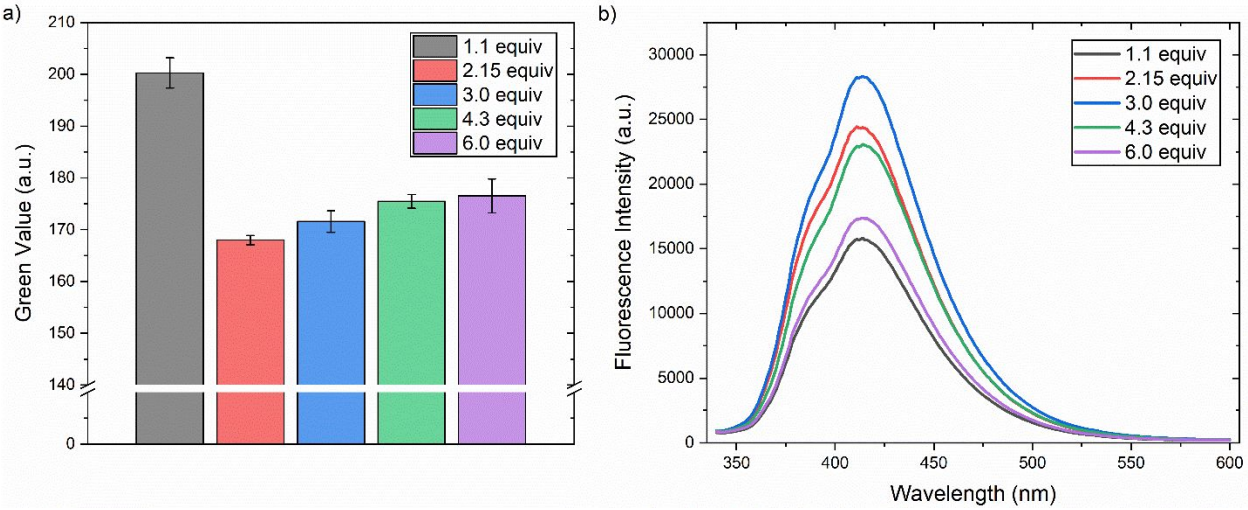

Figure S9. Comparison of DBU equivalents (with respect to *N*-(1-naphthyl)ethylenediamine) by a) colorimetric analysis and b) fluorescence spectroscopy. For colorimetric comparison, functionalized paper was treated with 300 µM sodium nitrite solution in ultrapure water. DBU: 1,8-diazabicyclo[5.4.0]undec-7-ene. Bars indicate error, i.e. standard deviation from three measurements.

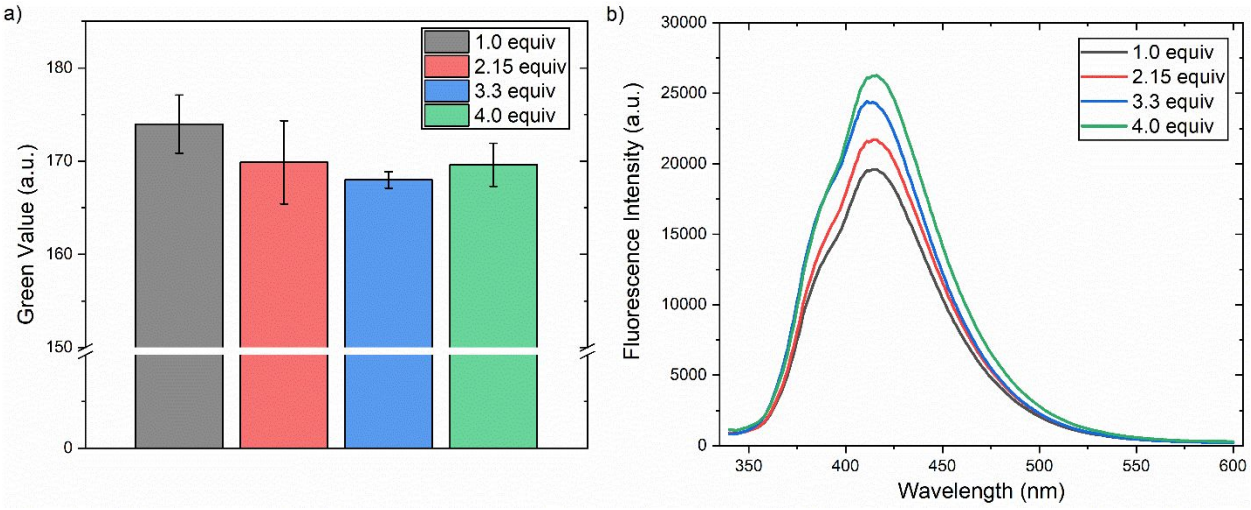

Figure S10. Comparison of epichlorohydrin equivalents (with respect to *N*-(1-napthyl)ethylenediamine) by a) colorimetric analysis and b) fluorescence spectroscopy. For colorimetric comparison, functionalized paper was treated with 300 µM sodium nitrite solution in ultrapure water. Bars indicate error, i.e. standard deviation from three measurements.

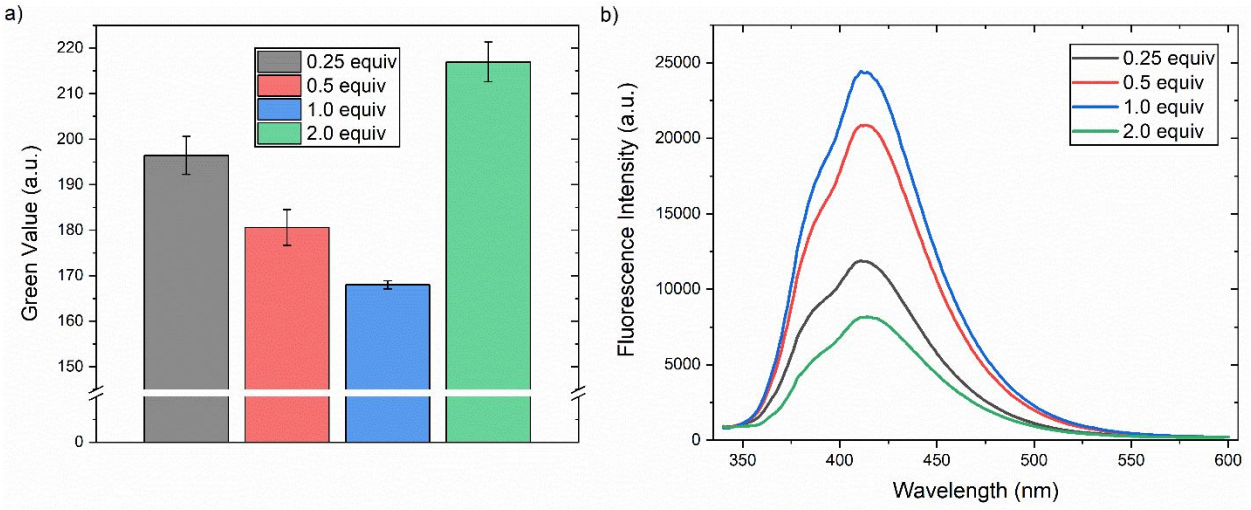

Figure S11. Comparison of *N*-(1-naphthyl)ethylenediamine equivalents (with respect to cellulose as glucose units) by a) colorimetric analysis and b) fluorescence spectroscopy. For colorimetric comparison, functionalized paper was treated with 300 µM sodium nitrite solution in ultrapure water. Bars indicate error, i.e. standard deviation from three measurements.

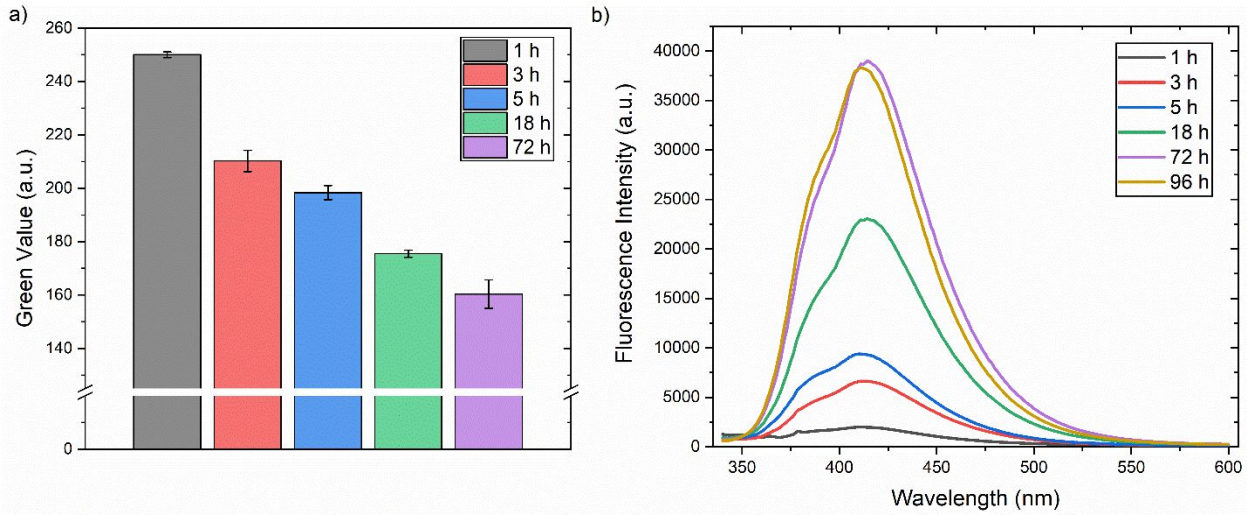

Figure S12. Comparison of reaction times for cellulose functionalization reaction by a) colorimetric analysis and b) fluorescence spectroscopy. For colorimetric comparison, functionalized paper was treated with 300 µM sodium nitrite solution in ultrapure water. Bars indicate error, i.e. standard deviation from three measurements.

Quantification of Functionalization Density – Fluorescence Calibration Curves

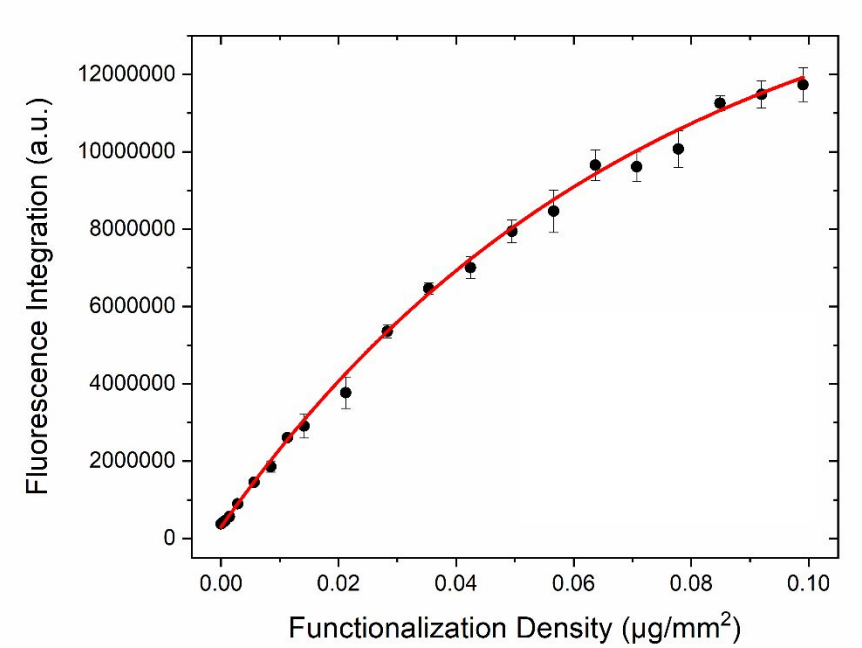

Figure S13. BioTek fluorescence calibration curve for degree of *N*-(1-naphthyl)ethylenediamine functionalization of Whatman 602h. An exponential curve model (red line) with an equation of: $y = A_1^{(-x/t)} + y_0$ was fit to the data where $A_1 = -15569867$ (± 582332); $t_1 = 0.07208$ (± 0.00392); $y_0 = 15864232$ (± 588103); and $R^2 = 0.99839$

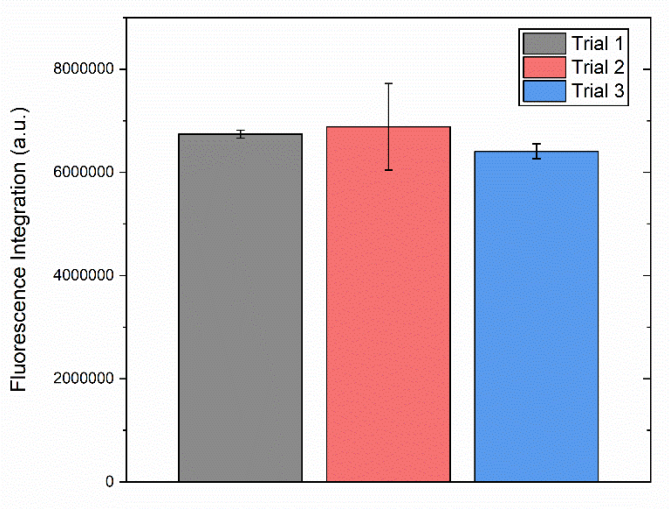

Figure S14. Reproducibility comparison of three separate cellulose functionalization trials by fluorescence spectroscopy.

Sensor Readout Optimization

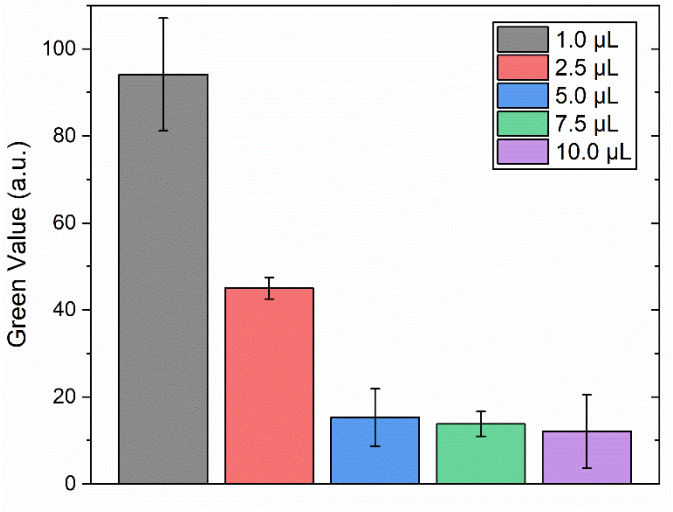

Figure S15. Colorimetric comparison, using 200 µM sodium nitrite in ultrapure water, of the amount of solution sulfanilamide solution (50 µM in 1.0 M phosphoric acid) required for optimal color development. 7.5 and 10.0 µL solutions degraded (decolored) faster than other conditions.

It was found that the identity and concentration of the acid in which sulfanilamide is dissolved and deposited onto the device is crucial for color development both in terms of lowest NGV (darkest color) and lowest PSD (lowest pixel heterogeneity). In some cases, lower NGV values promoted by stronger acids led to an increase in PSD, i.e. uneven detection zone coloration. Therefore, a variety of acids and acid mixes were analyzed and compared below. In the graphs below, the best acidic media is represented by both low NGV and low PSD values (i.e. closest to the bottom left of the graphs). Optimal paper functionalization and device fabrication procedures were used, and each device was treated with a 35 µM sodium nitrite solution.

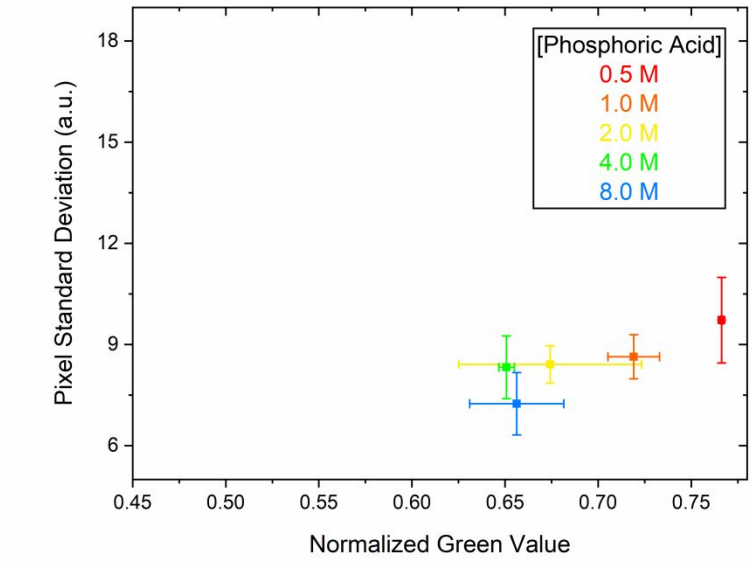

Figure S16. Comparison by Normalized Green Value and Pixel Standard Deviation of different concentrations of phosphoric acid media for sulfanilamide deposition.

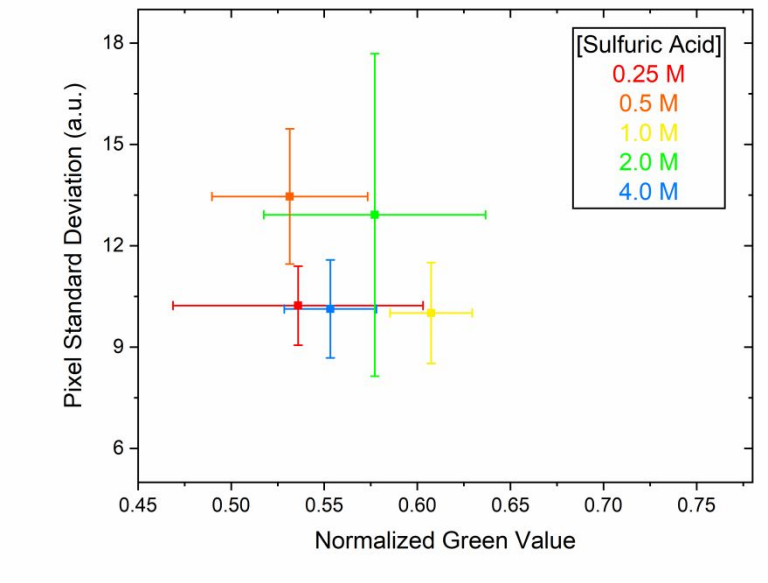

Figure S17. Comparison by Normalized Green Value and Pixel Standard Deviation of different concentrations of sulfuric acid media for sulfanilamide deposition.

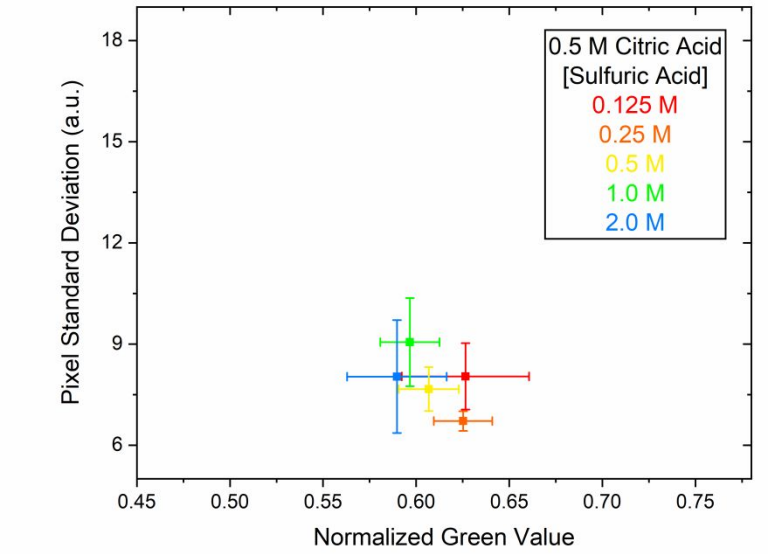

Figure S18. Comparison by Normalized Green Value and Pixel Standard Deviation of a mix of 0.5 M citric acid and different concentrations of sulfuric acid media for sulfanilamide deposition.

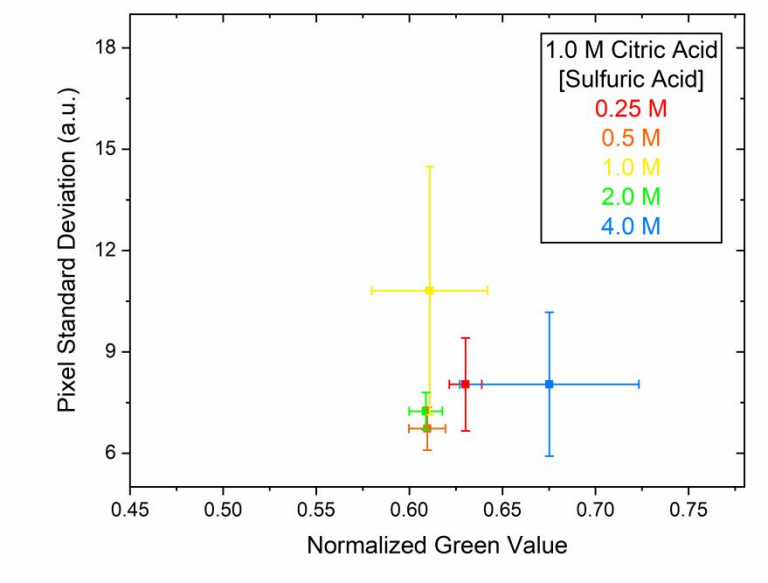

Figure S19. Comparison by Normalized Green Value and Pixel Standard Deviation of a mix of 1.0 M citric acid and different concentrations of sulfuric acid media for sulfanilamide loading

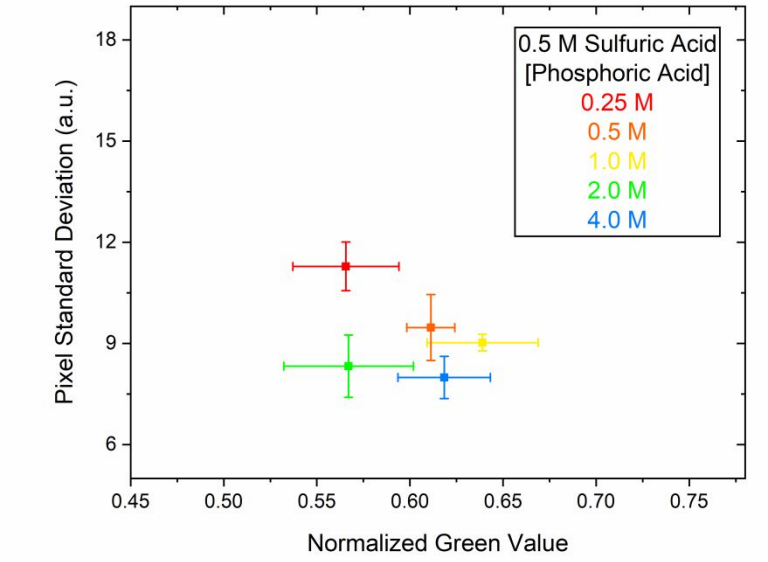

Figure S20. Comparison by Normalized Green Value and Pixel Standard Deviation of a mix of 0.5 M sulfuric acid and different concentrations of phosphoric acid media for sulfanilamide loading

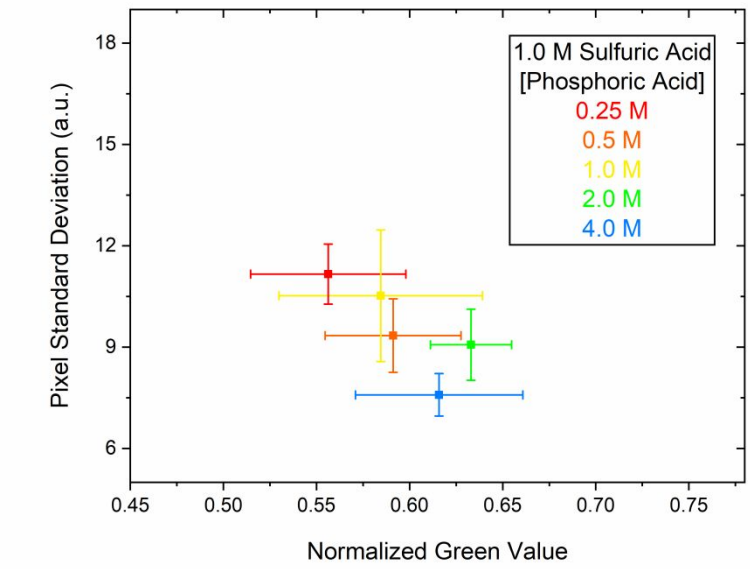

Figure S21. Comparison by Normalized Green Value and Pixel Standard Deviation of a mix of 1.0 M sulfuric acid and different concentrations of phosphoric acid media for sulfanilamide loading

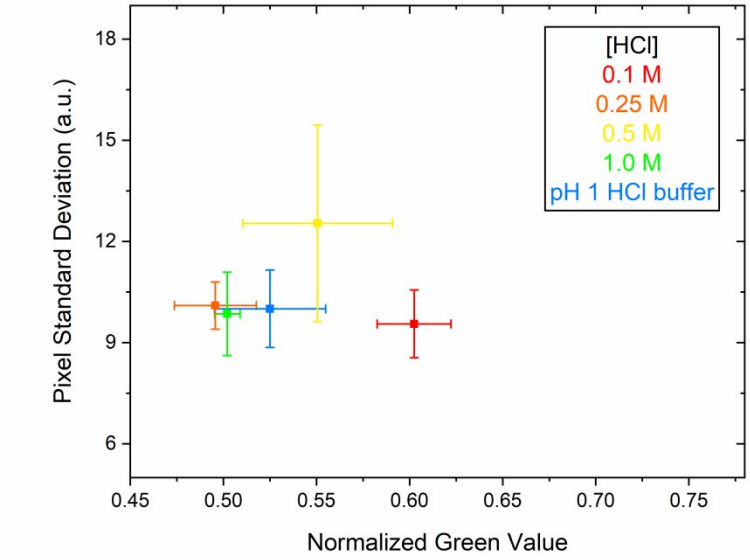

Figure S22. Comparison by Normalized Green Value and Pixel Standard Deviation of different concentrations of hydrochloric acid media for sulfanilamide loading

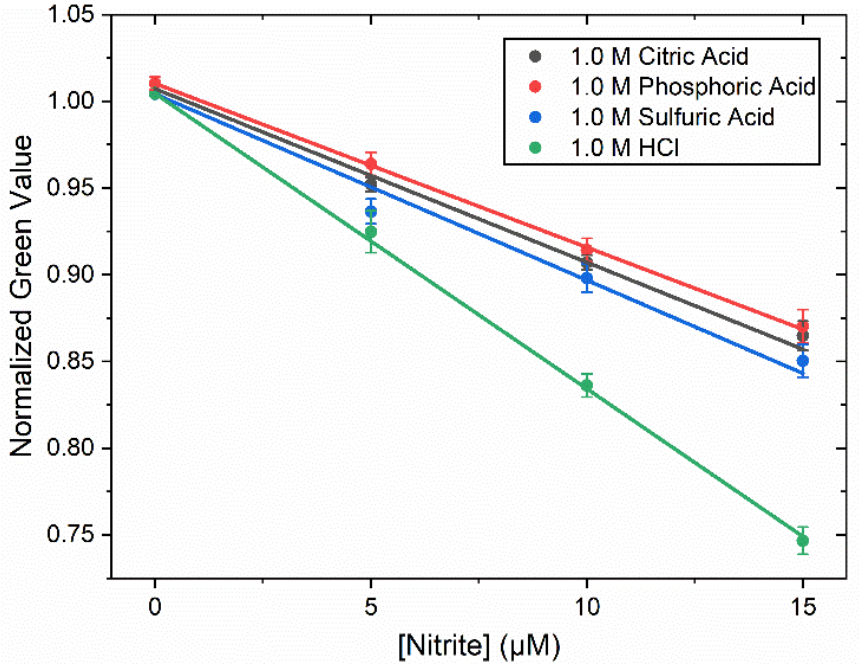

Figure S23. Comparison of nitrite detection calibration curves using different acidic media for sulfanilamide deposition

Limits of Detection and Quantitation

Limits of detection (LOD) and quantitation (LOQ) were calculated based on the average signals and standard deviations of the blank measurements for each individual calibration curve using the equations:[4]

$y_{LOD} = \bar{y}_B + 3\sigma_B$

$y_{LOQ} = \bar{y}_B + 10\sigma_B$

where y_{LOD} and y_{LOQ} are the signal responses corresponding to the system LOD and LOQ, $\bar{y}_B$ is the average signal response of the blank measurement, and σ_B is the standard deviation of the blank measurement. This signal response is then substituted for y into the best fit nonlinear equation to solve for the concentration of analyte (x) corresponding to the LOD and LOQ signal responses.

For linear systems with increasing trends where $\bar{y}_B = 0$ a.u (or can be normalized to 0 a.u.) this can be simplified using the linear equation $y = mx$ to $x_{LOD} = 3\sigma_B/m$ or $x_{LOQ} = 10\sigma_B/m$.

Table S1. Comparison of limits of detection (LODs) and limits of quantitation (LOQs) using different acidic conditions.

Acid (1.0 M)	LOD (μM)	LOQ (μM)
citric acid	0.84	3.33
phosphoric acid	1.05	3.81
sulfuric acid	0.42	0.77
hydrochloric acid	0.087	0.29

Table S2. Data for the nitrite detection calibration curve, in ultrapure water, for devices constructed using 50 mM sulfanilamide in 1.0 M citric acid solution

[Nitrite] (μM)	**NGV**	**NGV standard deviation**
0	1.01029	0.00379
5	0.95209	0.00405
10	0.90705	0.00424
15	0.86486	0.00847
20	0.81186	0.00434
25	0.78805	0.01659
30	0.74412	0.00936
35	0.71586	0.00762
40	0.70798	0.02041
45	0.60811	0.02184
50	0.6061	0.02285
55	0.60385	0.00702

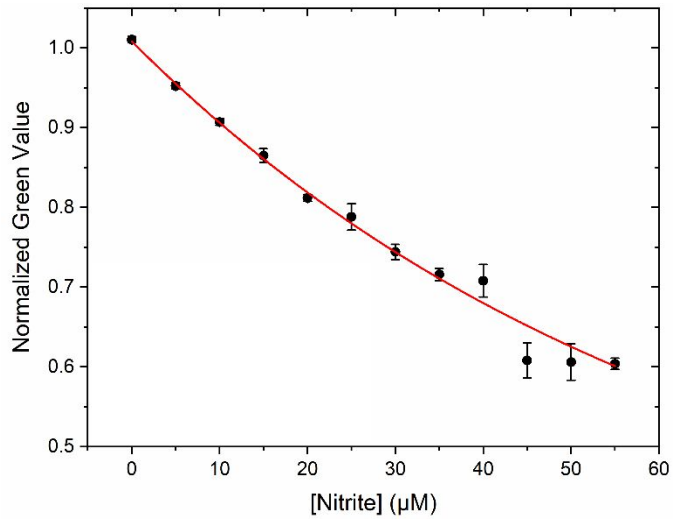

Figure S24. Nitrite calibration curve for devices constructed using 50 mM sulfanilamide in 1.0 M citric acid solution. The data were fit to an exponential decay curve: $y = A^{(-x/t)} + y_0$ where A = 0.70747 (±0.08594); t = 64.18914 (± 12.37246); y_0 = 0.30069 (± 0.09047); and R^2 = 0.99954. The LOD and LOQ values were calculated to be 0.84 μM and 3.33 μM, respectively

Table S3. Data for the nitrite detection calibration curve for devices constructed using 50 mM sulfanilamide in 1.0 M phosphoric acid solution

[Nitrite] (μM)	NGV	NGV standard deviation
0	1.01029	0.00379
5	0.96389	0.00674
10	0.91415	0.00677
15	0.87027	0.00973
20	0.81629	0.0214
25	0.77817	0.00766
30	0.74307	0.00946
35	0.70012	0.00911
40	0.68379	0.00203
45	0.63408	0.05899
50	0.61447	0.00816
55	0.56796	0.00354

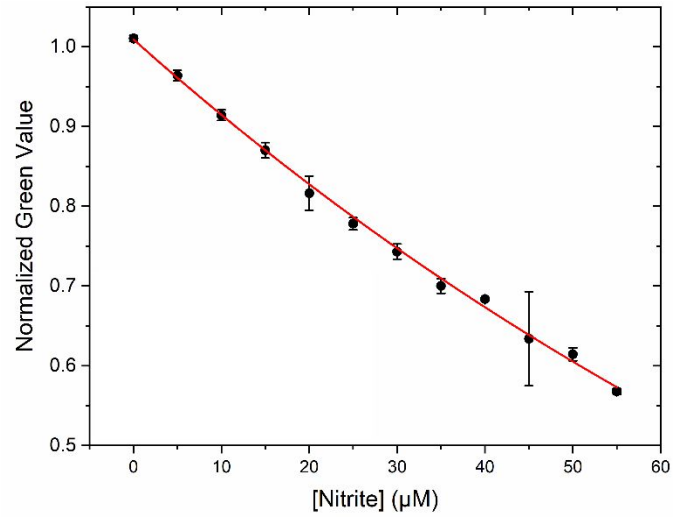

Figure S25. Nitrite calibration curve for devices constructed using 50 mM sulfanilamide in 1.0 M phosphoric acid solution. The data were fit to an exponential decay curve: $y = A^{(-x/t)} + y_0$ where A = 1.20451 (±0.23337); t = 122.40866 (± 30.21403); y_0 = -0.19526 (± 0.23678); and R^2 = 0.99978. The LOD and LOQ values were calculated to be 1.05 μM and 3.81 μM, respectively

Table S4. Data for the nitrite detection calibration curve for devices constructed using 50 mM sulfanilamide in 1.0 M sulfuric acid solution.

[Nitrite] (μM)	NGV	NGV standard deviation
0	1.00432	0.00065
5	0.9365	0.00711
10	0.89807	0.00821
15	0.85037	0.00943
20	0.77369	0.00711
25	0.7086	0.02046
30	0.69304	0.03974
35	0.66724	0.02178
40	0.62579	0.02491
45	0.5849	0.03419
50	0.59666	0.03147
55	0.51248	0.03841

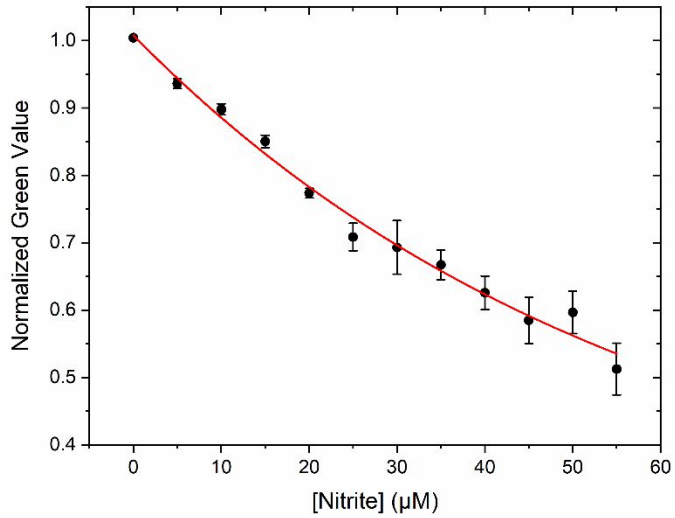

Figure S26. Nitrite calibration curve for devices constructed using 50 mM sulfanilamide in 1.0 M sulfuric acid solution. The data were fit to an exponential decay curve: $y = A^{(-x/t)} + y_0$ where A = 0.7709 (±0.14399); t = 57.91361 (± 15.96034); y_0 = 0.23713 (± 0.14918); and R^2 = 0.99953. The LOD and LOQ values were calculated to be 0.42 μM and 0.77 μM, respectively

Table S5. Data for the nitrite detection calibration curve for devices constructed using 50 mM sulfanilamide in 1.0 M HCl solution.

[Nitrite] (μM)	NGV	NGV standard deviation
0	1.00455	0.00050
5	0.92475	0.01203
10	0.83622	0.00678
15	0.74663	0.00782
20	0.71671	0.00605
25	0.63506	0.03251
30	0.56766	0.01194
35	0.50206	0.00686
40	0.48787	0.01326
45	0.39869	0.0051
50	0.37175	0.03668
55	0.28689	0.05198

Table S6. Data for the nitrite detection calibration curve for devices constructed using 50 mM sulfanilamide solution in a mixture of 1.0 M citric acid and 0.25 M sulfuric acid

[Nitrite] (µM)	NGV	NGV standard deviation
0	1.003252	0.000384
5	0.934942	0.003073
10	0.881022	0.003107
15	0.819796	0.033176
20	0.737478	0.019568
25	0.708931	0.006568
30	0.630364	0.037578
35	0.626183	0.01016
40	0.548602	0.033031
45	0.486057	0.061036
50	0.446383	0.053046
55	0.386995	0.163772

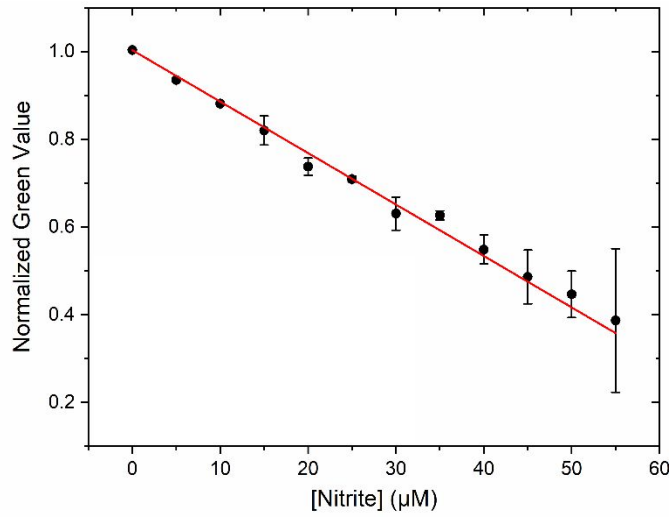

Figure S27. Nitrite calibration curve for devices constructed using 50 mM sulfanilamide solution in a mix of 1.0 M citric acid and 0.25 M sulfuric acid. The data were fit to a linear curve: y = mx + b where m = -0.01173 (±0.0002475); b = 1.00307 (± 0.00062108); and R^2 = 0.99557. The LOD and LOQ values were calculated to be 0.098 µM and 0.33 µM, respectively

Table S7. Data for the nitrite detection calibration curve, from 5 – 87.5 µM, in synthetic freshwater for devices constructed using the optimal methods.

[Nitrite] (µM)	NGV	NGV standard deviation
0	1.00391	6.91866E-4
5	0.90982	0.01344
10	0.8426	0.00846
15	0.75805	0.03182
20	0.72225	0.02546
25	0.69703	0.04034
30	0.61046	0.01583
35	0.56402	0.03024
40	0.54325	0.03469
45	0.51168	0.02542
50	0.44733	0.04462
62.5	0.37719	0.053
75	0.2487	0.05894
87.5	0.22507	0.03786

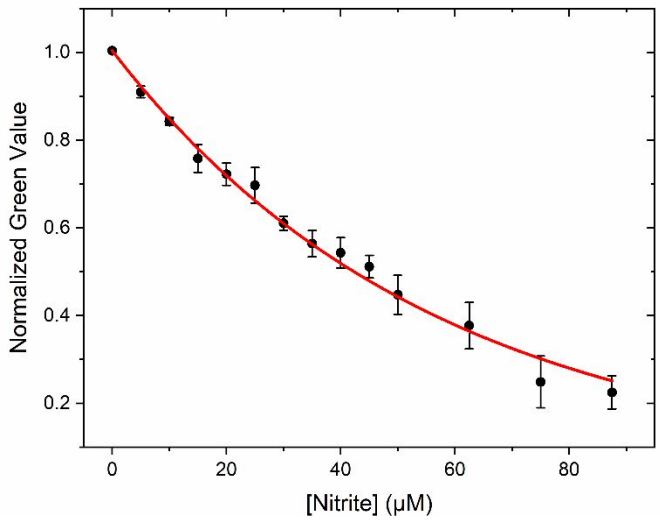

Figure S28. Nitrite calibration curve, from 5 to 87.5 µM, in synthetic freshwater, for devices constructed using the optimal conditions. The data were fit to an exponential decay curve: $y = A^{(-x/t)} + y_0$ where A = 0.995562 (± 0.06177); t = 56.53845 (± 5.21821); y_0 = 0.04824 (± 0.0619); and R^2 = 0.99783. The LOD and LOQ values were calculated to be 0.12 µM and 0.41 µM respectively

Table S8. Data for the nitrite detection calibration curve, from 0.05 – 5 µM, in synthetic freshwater for devices constructed using the optimal methods.

[Nitrite] (µM)	NGV	NGV standard deviation
0	1.00255	0.00156
0.05	1.00242	0.00132
0.1	1.00262	0.00168
0.25	1.00136	0.00101
0.5	0.99421	0.00217
0.75	0.99138	0.00163
1	0.98904	0.00214
1.25	0.97882	0.00326
1.5	0.97624	0.00525
2	0.96799	0.00654
3.5	0.94018	0.01057
5	0.91561	0.0159

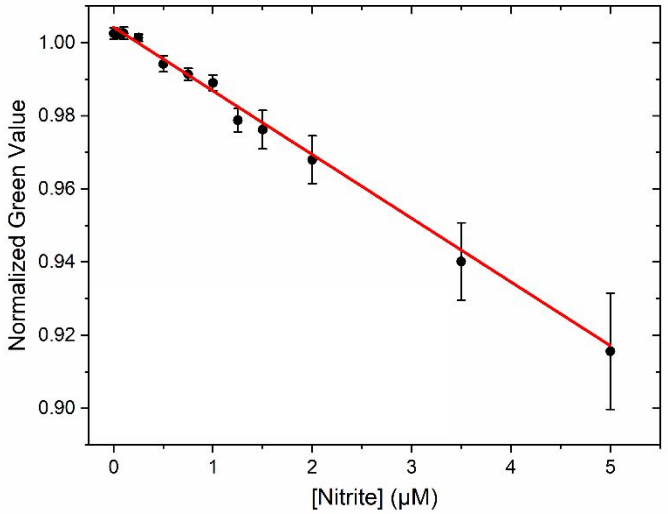

Figure S29. Nitrite calibration curve, from 0.05 to 5 µM, in synthetic freshwater, for devices constructed using the optimal conditions. The data were fit to a linear curve: y = mx +b, where m = -0.017422 (± 0.00102); b = 1.00426 (± 0.00058537); and R^2 = 0.96675. The LOD and LOQ values were calculated to be 0.26 µM and 0.69 µM respectively

Table S9. Data for the nitrite detection calibration curve, from 5 – 50 µM, in Sargasso seawater for devices constructed using the optimal methods

[Nitrite] (µM)	NGV	NGV standard deviation
0	0.99995	0.00135
5	0.86101	0.01602
10	0.7553	0.01126
15	0.64813	0.01458
20	0.56135	0.0305
25	0.51689	0.07002
30	0.41377	0.09217
35	0.31187	0.05733
40	0.15831	0.0542
45	0.13339	0.04322
50	0.05295	0.0233

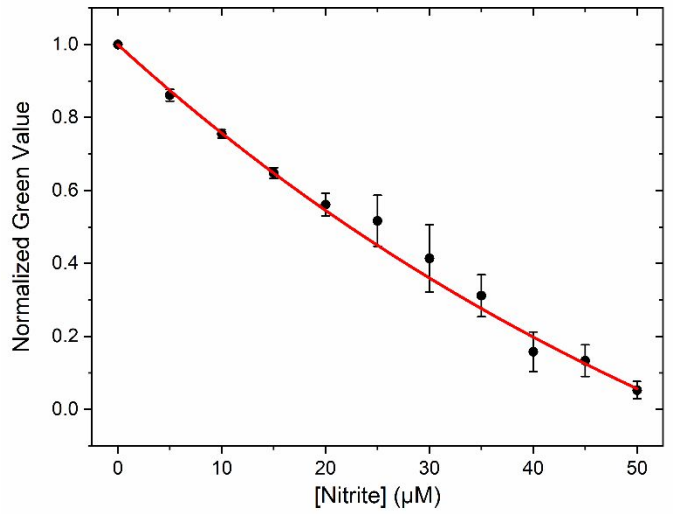

Figure S30. Nitrite calibration curve, from 5 to 50 µM, in Sargasso seawater, for devices constructed using the optimal conditions. The data were fit to an exponential decay curve: $y = A^{(-x/t)} + y_0$ where A = 1.92658 (± 0.15965); t = 74.37635 (± 7.79546); y_0 = -0.9267 (± 0.15972); and R^2 = 0.99918. The LOD and LOQ values were calculated to be 0.15 µM and 0.52 µM respectively

Table S10. Data for the nitrite detection calibration curve, from 0.05 – 5 µM, in Sargasso seawater for devices constructed using the optimal methods.

[Nitrite] (µM)	NGV	NGV standard deviation
0	0.99667	0.00257
0.05	0.99153	8.18304E-4
0.1	0.99347	0.00158
0.25	0.99055	0.00201
0.5	0.98472	0.00109
0.75	0.97633	0.00238
1	0.96111	0.0066
1.25	0.95035	0.00565
1.5	0.94326	0.00641
2	0.92775	0.00987
3.5	0.90033	0.0112
5	0.85462	0.01256

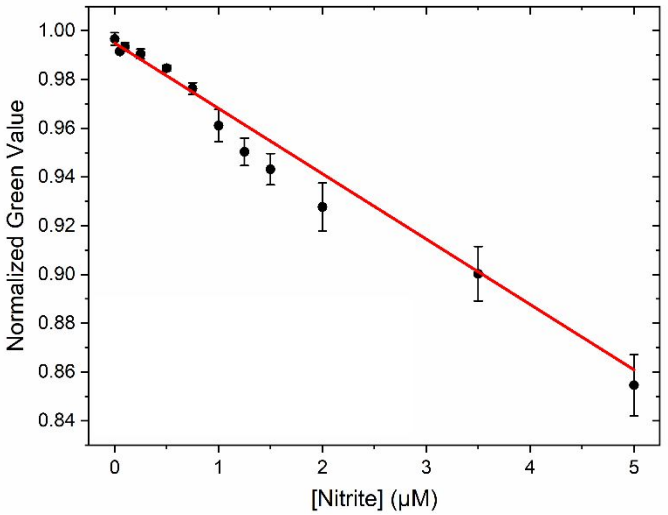

Figure S31. Nitrite calibration curve, from 0.05 to 5 µM, in Sargasso seawater, for devices constructed using the optimal conditions. The data were fit to a linear curve: y = mx +b, where m = -0.0268 (± 0.00233); b = 0.995 (± 0.0011); and R^2 = 0.92972. The LOD and LOQ values were calculated to be 0.22 µM and 0.89 µM respectively

Interference Studies

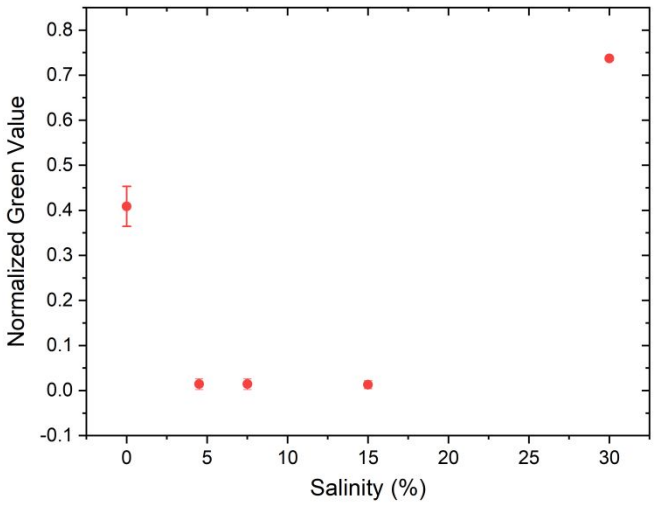

Figure S32. Comparison of sensor readout for samples of 50 μM nitrite in high percent salinity solutions

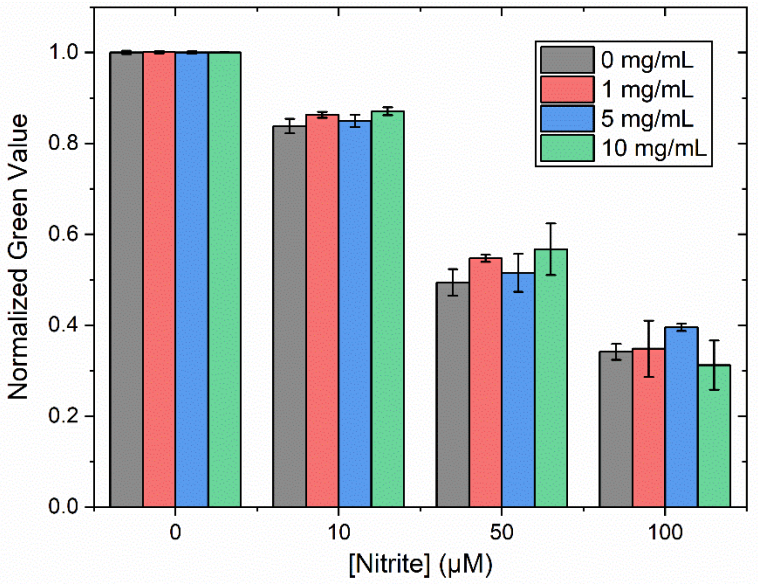

Figure S33. Comparison of sensor readouts for nitrite concentrations of 0, 10, 50, or 100 μM in solutions of various turbidities (mg/mL) created using Kaolin clay

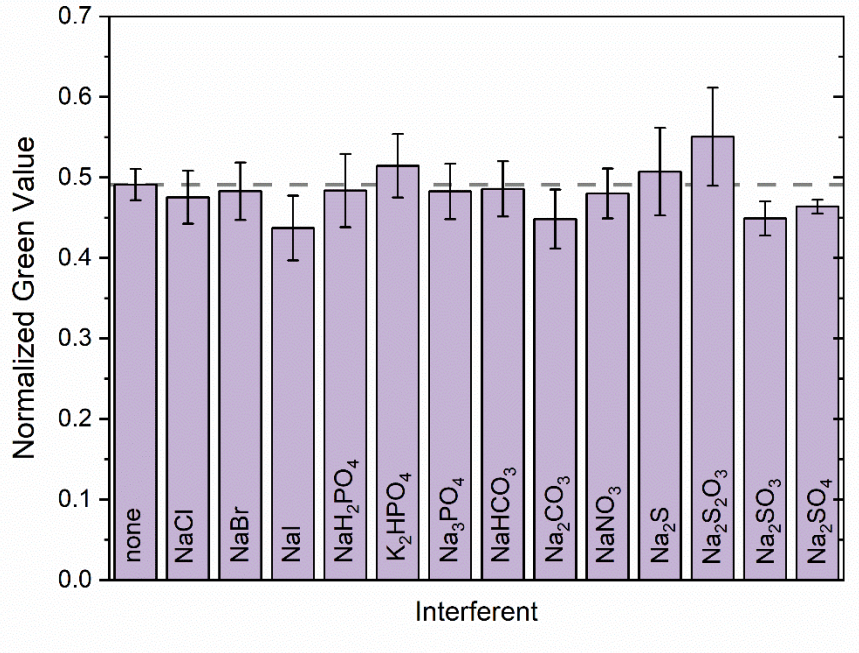

Figure S34. Comparison of sensor readouts for samples containing 50 μM sodium nitrite and 50 μM potential interferent anion

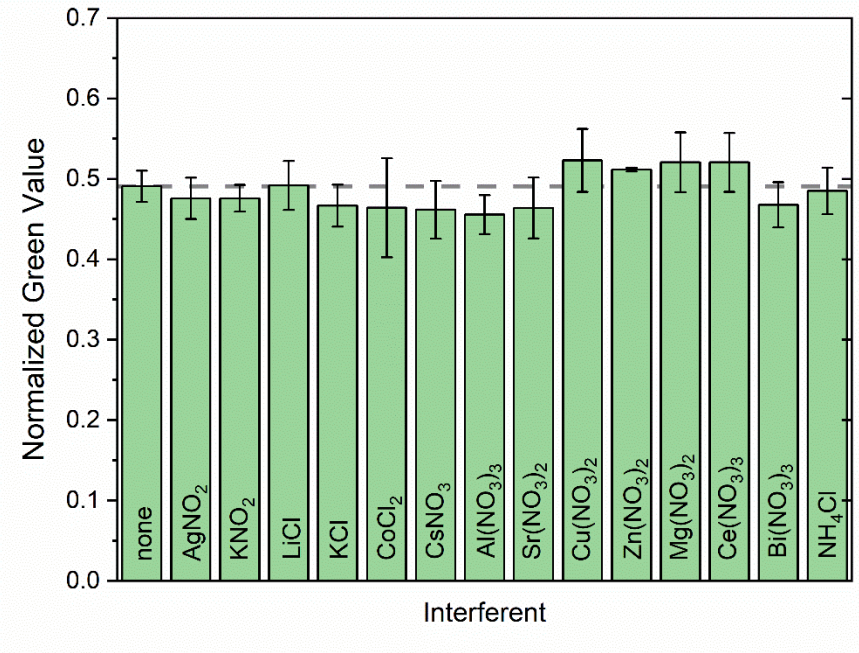

Figure S35. Comparison of sensor readouts for samples containing 50 μM sodium nitrite and 50 μM potential interferent cation. Alternative nitrite salts ($AgNO_2$ and KNO_2) did not contain sodium nitrite.

Real-World Samples

Figure S36. Picture of actual, unfiltered samples from the Houston Hurricane Harvey flood waters (from left to right: downtown Houston, 5 miles northwest of Houston, and 5 miles southeast of Houston) analyzed with the reported device

Sensor Longevity

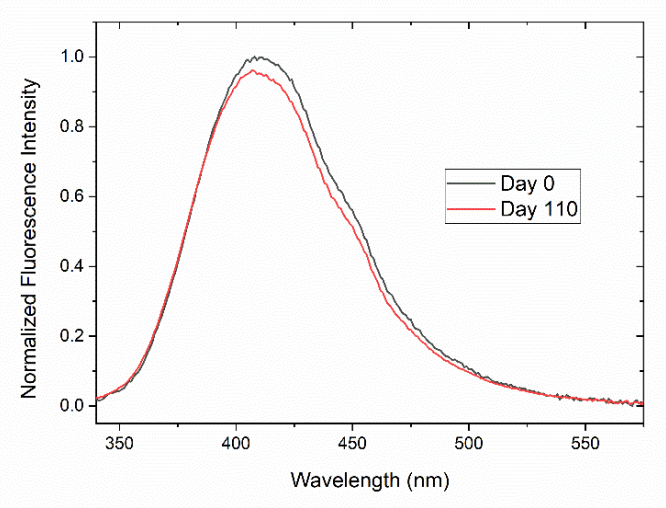

Figure S37. Comparison of the fluorescence of functionalized paper when first synthesized (day 0) and 110 days later

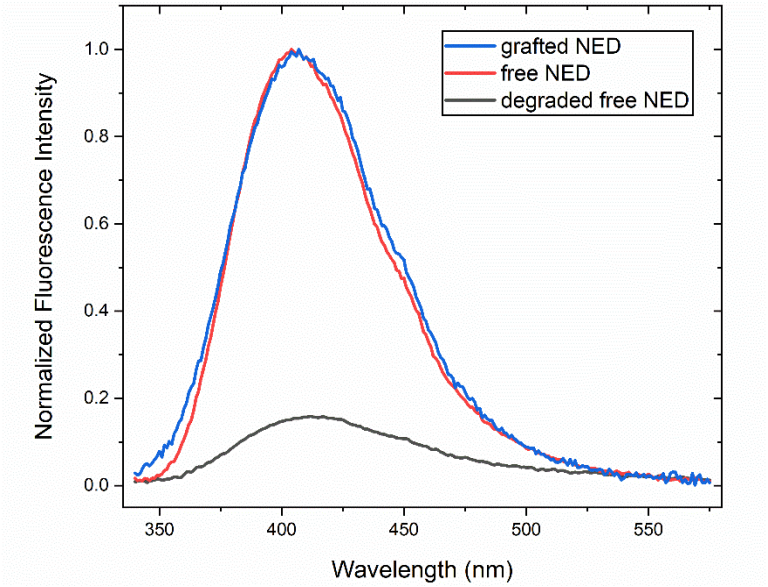

Figure S38. Fluorescence comparison of cellulose functionalized with *N*-1(naphthyl)ethylenediamine (grafted NED, blue line) to free NED dried on cellulose before (red line) and after (grey line) degradation for 5 hours under UV light in open air.

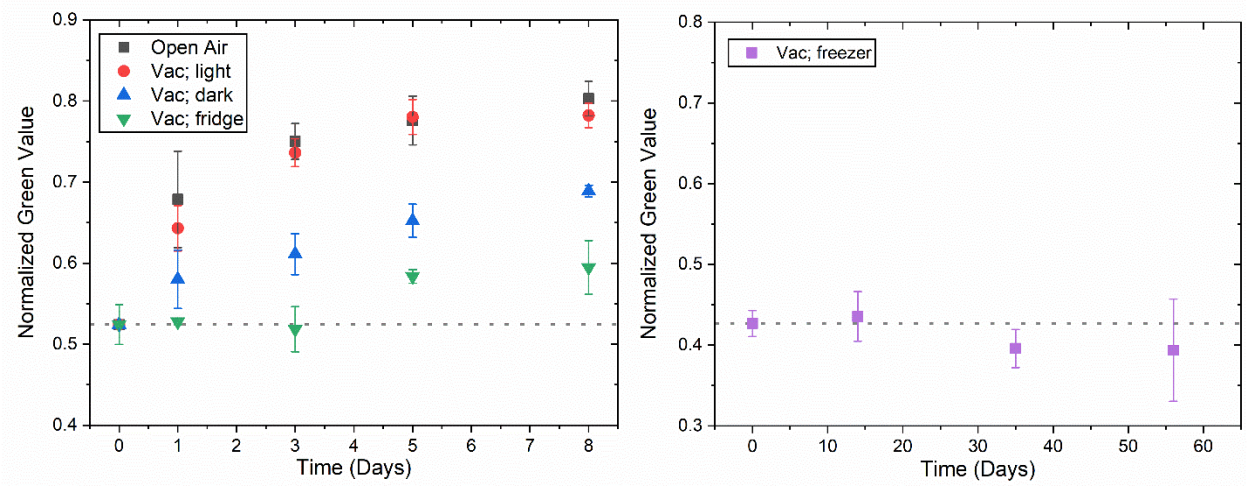

Figure S39. Comparison of sensor readout, using 50 µM nitrite solution, after storage in different conditions: open air with ambient light and temperature (grey), vacuum with ambient light and temperature (red), vacuum with darkness and ambient temperature (blue), and vacuum with darkness at ≤ 4 °C (green), and vacuum with darkness at ≤ -20 °C.

References

[1] Methods for Measuring the Acute Toxicity of Effluents and Receiving Waters to Freshwater and Marine Organisms. *United States Environmental Protection Agency*, 5th ed. EPA-821-r-02-012; USEPA Office of Water: Washington, DC, 2002; pp 32-34

[2] Fawcett, S. E.; Johnson, K. S.; Riser, S. C.; Van Oostende, N.; Sigman, S. M. Low-Nutrient Organic Matter in the Sargasso Sea Thermocline: A Hypothesis for its Role, Identity, and Carbon Cycle Implications. *Marine Chem.* **2018**, *27*, 108-123.

[3] Pozor, M.; Morrissey, H.; Albanese, V.; Khouzam, N.; Deriberprey, A.; Macpherson, M. L.; Kelleman, A. A. Relationship between Echotextural and Histomorphometric Characteristics of Stallion Tests. *Theriogernology* **2017**, *99*, 134-145.

[4] Belter, M.; Sajnóg, A.; Barałkiewicz, D. Over a Century of Detection and Quantification Capabilities in Analytical Chemistry – Historical Overview and Trends. *Talanta* **2014**, *129*, 606-616.